

## Research Article

# Improving Ballistic Performance of Polyurethane Foam by Nanoparticle Reinforcement

M. F. Uddin,<sup>1</sup> H. Mahfuz,<sup>2</sup> S. Zainuddin,<sup>3</sup> and S. Jeelani<sup>3</sup>

<sup>1</sup> School of Aeronautics and Astronautics, Purdue University, West Lafayette, IN 47907, USA

<sup>2</sup> Department of Ocean and Mechanical Engineering, Florida Atlantic University, Boca Raton, FL 33431, USA

<sup>3</sup> Tuskegee University's Center for Advanced Materials, Tuskegee, AL 36088, USA

Correspondence should be addressed to H. Mahfuz, hmahfuz@fau.edu

Received 7 August 2009; Accepted 5 November 2009

Recommended by Simon Joseph Antony

We report improving ballistic performance of polyurethane foam by reinforcing it with nanoscale TiO<sub>2</sub> particles. Particles were dispersed through a sonic cavitation process and the loading of particles was 3 wt% of the total polymer. Once foams were reinforced, sandwich panels were made and impacted with fragment simulating projectiles (FSPs) in a 1.5-inch gas gun. Projectile speed was set up to have complete penetration of the target in each experiment. Test results have indicated that sandwich with nanophased cores absorbed about 20% more kinetic energy than their neat counterpart. The corresponding increase in ballistic limit was around 12% over the neat control samples. The penetration phenomenon was also monitored using a high-speed camera. Analyses of digital images showed that FSP remained inside the nanophased sandwich for about 7 microseconds longer than that of a neat sandwich demonstrating improved energy absorption capability of the nanoparticle reinforced core. Failure modes for energy absorption have been investigated through a microscope and high-speed images.

Copyright © 2009 M. F. Uddin et al. This is an open access article distributed under the Creative Commons Attribution License, which permits unrestricted use, distribution, and reproduction in any medium, provided the original work is properly cited.

## 1. Introduction

The obvious attraction of sandwich structures such as light weight and a high bending stiffness is strongly influenced by the core material. The core material should be as light as possible and should act as a spacer for the stiff skins to increase the moment of inertia. It plays an important role to improve the structural crashworthiness as they are capable of absorbing large amounts of energy in the event of impact [1, 2]. However, the resulting impact damage to the sandwich panel ranges from facesheet indentation to complete perforation. One of the most commonly used parameter to quantify short-duration impact phenomenon is the ballistic limit. The ballistic limit is defined as the greatest projectile velocity that a target can withstand without being perforated by the projectile [3]. Many researchers have studied sandwich structures with special emphasis on the facesheets [4–6]. Lee and Sun [4] studied graphite/epoxy laminate impacted by standard projectiles. They concluded three stages of penetration process—predeformation, postdeformation before plugging, and postplugging. However,

the situation is somewhat different in case of core materials. Goldsmith et al. [7] reported that the location of initial contact point is a critical issue for impact in core materials. When the first contact occurred along a cell axis, cell wall resulted in an out-of-plane deformation followed by in-plane distortion after the striker moved to a more central position during the course of the perforation. However the effect of the location of initial contact is substantially reduced when the size of the striker is much larger than that of the cell. Extensive studies were reported on perforation of sandwich structures impacted by projectiles [8, 9].

While numerous studies focused on facesheet or composites under ballistic impact, the study of foam core remains scarce. In the present investigation, efforts have been made to improve the ballistic performance of sandwich by improving the core properties. In our previous work, the rigid polyurethane foam was modified by infusing nanoparticles [10]. The modified foam showed improved mechanical properties both in static and dynamic compression tests. The effect was even more pronounced when this modified foam was used as core materials for sandwich structures [11]. A

few more attempts have been made to infuse nanoparticles in polyurethane and reported enhancement in chemical and mechanical properties [12–16]. Cao et al. [12, 13] reinforced polyurethane foam with the inclusion of 5% functional organoclay and reported improved glass transition temperature and mechanical properties of polyurethane foam with 5% nanoclay. Petrović et al. [15] and Javni et al. [16] studied the effect of nanosilica and microsilia fillers on polyurethane foam properties. They reported that hardness and compressive strength of flexible polyurethane foams with nanosilica were increased while decreased with microsilia fillers. One special advantage of infusing nanoparticles is that only a small amount of nanoparticles, typically 1–3 wt%, is required in order to achieve this enhancement and, hence, eliminating the weight penalty due to the reinforcement. However, the unique nanocomposite features can only be effective if the nanoparticles are well dispersed on a nanometer level in the surrounding polymer matrix [17]. Various techniques are available to infuse nanoparticle in the polymer matrices [18] among which sonication is one of the efficient ways to disperse nanoparticles into the virgin materials as reported by the authors elsewhere [19, 20]. Moreover, there is a clear acceleration of polyurethane polymerization reaction under ultrasound in both catalyzed and uncatalyzed reactions [21]. As modified nanophased foam core and their sandwich showed superior performance both in static and dynamic compression, the work was extended to investigate their performance under ballistic loading as well as to understand their failure mechanisms and penetration process.

## 2. Experimental

**2.1. Materials.** The materials used for manufacturing the sandwich composite with nanophased foam are shown in Table 1. Manufacturing procedure of sandwich composites with nanophased core is discussed elaborately in our previous work [11]. However, in brief, nanophased polyurethane foam was fabricated in two steps—the first step was the dispersion of nanoparticles (via sonication) into liquid polyurethane, and the second was the casting of foam. Once the core is made, the coinjection resin transfer molding (CIRTM) technique was employed to fabricate the sandwich panels. Two types of sandwiches were manufactured, one with neat polyurethane core and the other with nanophased polyurethane core. Several panels were fabricated in this manner, and samples are extracted for subsequent tests.

**2.2. Microstructural Tests.** SEM analyses were carried out using JEOL JSM 5800. As-prepared neat and nanophased polyurethane foam samples were placed on a sample holder with a silver paint and coated with gold palladium to prevent charge build-up by the electron. A 15-kilovolt accelerating voltage was applied to accomplish desired magnification.

**2.3. High-Velocity Impact Test.** A 1.5-inch gas gun with 22 ft long barrel was used to perform the high-velocity impact test (Figure 1(a)). The projectile used was a 13 gm, 12.7 mm diameter fragment simulating projectile (FSP) made from

TABLE 1: Various materials used for making sandwich with nanophased foam.

Components	Materials	Vendors
Face sheet	Fiber: plane weave S2-glass 3 layers/facesheet	Owens Corning [22]
	Matrix: SC-15 Epoxy	Applied Poleramic Inc [23]
Foam materials	Diphenylmethane diisocyanate (part-A) Polyol (part B) Density: 240 kg/m <sup>3</sup>	Utah Foam Products [24]
	Nanoparticles 3-wt% TiO <sub>2</sub> Dia: 29-nm, Spherical shape	Nanophase Technologies Co. [25]

a hardened 4340 steel rod as shown in Figure 1(b). The FSP was carried by modulun sabot along the barrel. At the end of the gun barrel (muzzle), there was a 2-inch thick stripper plate with a center hole which stopped the sabot but allowed the projectile to continue. Two different types of magnetic sensors were used to record the impact velocity prior to impact and residual velocity after penetration. The gun is capable of firing FSP in the velocity range up to about 1000 m/s with helium gas.

**2.4. High-Speed Camera.** The IMACON 468 camera was used to take the images of projectiles during the penetration process. The camera is capable of taking 100 million frames per second and it includes a data reduction package (IMACON 468 software) from which velocity, distance, area, displacement, and angles can be extracted. For triggering, a break wire is placed in the path of the projectile at the end of the barrel (muzzle). On its passage towards the target (specimen), the projectile intersected the break wire which triggered the camera. A schematic view of the experimental setup is shown in Figure 2. According to Figure 2, delay time, interframe time, and exposure time were calculated to setup the camera such that it takes the successive images from the view field.

## 3. Results and Discussions

**3.1. Microstructural Properties.** In order to investigate the microstructural effect due to nanoparticles infusion. SEM analyses were carried out on both the neat and nanophased polyurethane foam. The micrographs of neat and nanophased foams at same magnification are shown in Figures 3(a) and 3(b). As seen in Figures 3(a) and 3(b), cell edges and walls are distinctly visible with almost uniform cell structures throughout. The cell sizes are found to be larger for the nanophased polyurethane foam as compared to neat foam. The average cell sizes are found to be approximately 114  $\mu\text{m}$  for the neat foam and 167  $\mu\text{m}$  for the nanophased foam. With this significant enhancement in cell size, the

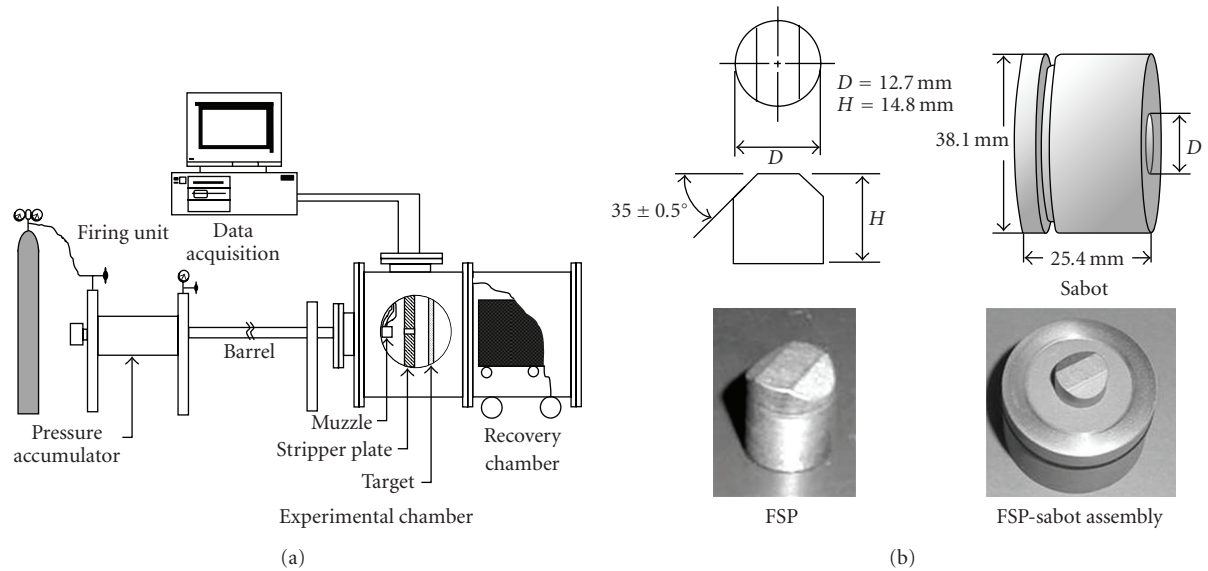


FIGURE 1: (a) Experimental setup for gas gun. (b) Projectile and sabot.

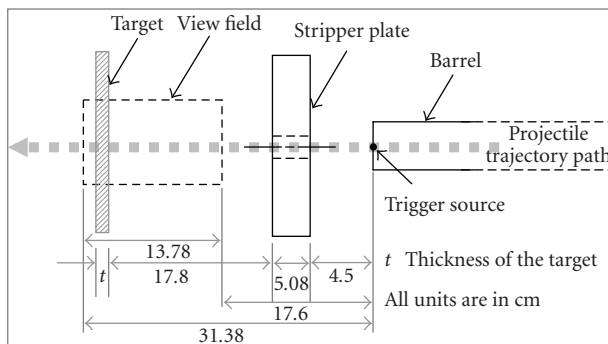


FIGURE 2: Experimental setup of gas gun with high-speed camera.

cell structure still seems to be intact and uniform. In polyurethane foam manufacturing, water is used as a main reactant to produce the blowing agent. Water reacts with the isocyanate group to generate the blowing gas  $\text{CO}_2$ . It is believed that infusion of nanoparticles acts as a catalyst to increase the kinetic rate of this chemical reaction. The increased kinetic rate helps the blowing gas to generate gradually and thus giving larger cell size [26].

As both neat and nanophased foams have similar densities [11] and they are fabricated in identical closed molds, nanophased foam with larger cell size must have thicker cell edge, wall, or faces than those of the neat foam. This is confirmed by SEM micrographs shown in Figure 4 where it is found that cell wall thickness in nanophased foam is  $7.4 \mu\text{m}$  whereas in neat polyurethane foam, it is  $3.86 \mu\text{m}$ . Also, the cross-sectional areas of cell edges were approximated as  $296 \mu\text{m}^2$  for neat and  $444 \mu\text{m}^2$  for nanophased foam. Due to the nanoparticle infusion, the cell wall and cell edge cross-section have increased by about 92% and 50%, respectively, in the nanophased foam.

**3.2. Ballistic Performance.** In this study, sandwiches with both neat and nanophased polyurethane foam core were impacted by a fragment simulating projectile at around 800 m/s velocity. The striking velocities were maintained at about 800 m/s by controlling the breech pressure which was kept at about 500 psi in all tests. The striking velocity was well above the ballistic limit of the material and complete piercing of the target occurred during the test. Figure 5 shows the relation between the striking velocity and the residual velocity for both neat and nanophased sandwich structures. The curves show a linear relation which is typical if the striking velocity exceeds the ballistic limit [7]. It is also observed that the neat sandwich shows higher residual velocity than the nanophased sandwich. This indicates that after complete perforation of the target, the projectile came out with higher kinetic energy in neat sandwich as compared to nanophased sandwich.

To investigate the above fact, the energy absorption by the target and ballistic limit were calculated using the principle of conservation of energy. The as-calculated energy absorption and ballistic limit for both neat and nanophased sandwiches are tabulated in Table 2. The parameters were normalized by areal density. The nanophased sandwich showed about 20% improvement in energy absorption whereas in case of ballistic limit, the enhancement was 12%.

**3.3. Failure Mechanisms.** In the event of high-velocity impact, when the projectile strikes the target, strong compressive waves propagate into both bodies. If the impact velocity is sufficiently high, relief waves will propagate inward from the lateral-free surface of the projectile and cross at the centerline, creating a region with high-tensile stress. On the other hand, when the initial compressive wave reaches a free boundary in the target, an additional release wave is generated. Any of these above waves may initiate failure in

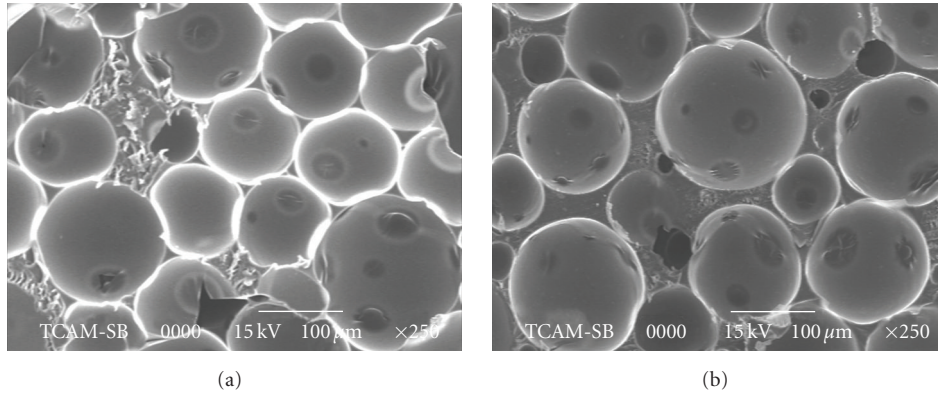


FIGURE 3: Microstructures of (a) neat (b) nanophased polyurethane foams.

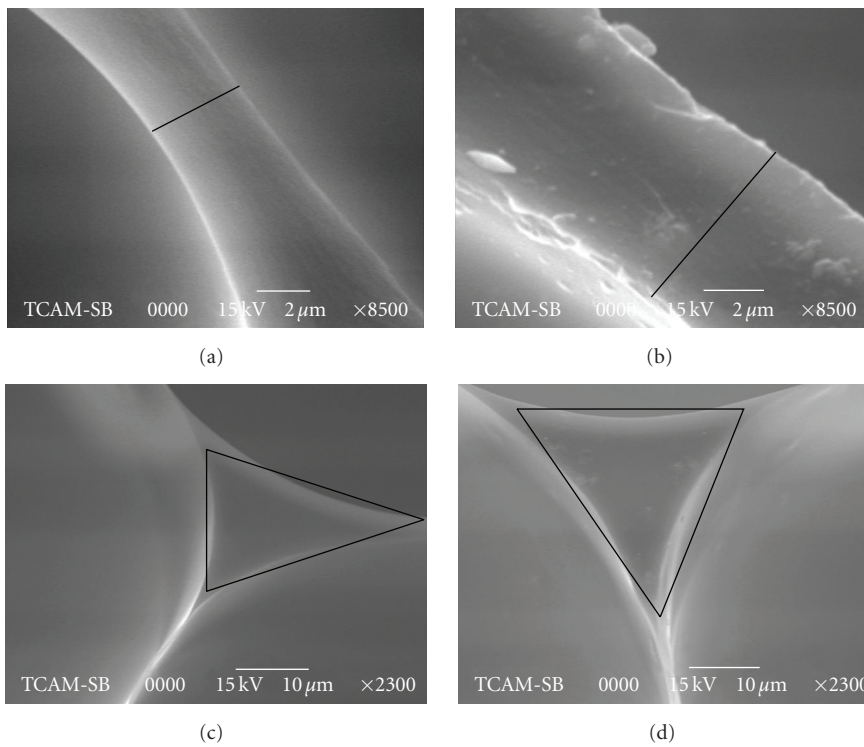


FIGURE 4: Cell walls of (a) neat and (b) nanophased polyurethane foam and cross-section of cell edges of (c) neat and (d) nanophased polyurethane foams.

the target and may trigger different failure modes. However, the wave propagation and, hence, the failure mechanisms depend on material properties, impact velocity, projectile shape, method of target support, and relative dimensions of projectile and target [27]. Some of the dominant failure modes for thin and intermediate thickness targets have been reported by Backman and Goldsmith [3]. Although one of these may dominate the failure process, they might frequently be accompanied by several other modes.

In the present study, the cores were investigated after penetration with a low-magnification optical microscope to analyze their failure mechanisms. Figure 6 shows the images of penetrated targets for both neat and nanophased sandwich

cores. It was observed that in both neat and nanophased cores, the most dominating failure mode was fragmentation leaving a crater at the center of the target. The diameter of the crater is equal to that of the impactor both in front and back side of the neat core. On the other hand, the crater diameter is equal to the impactor diameter at the front side but larger in the back side. This type of fragmentation is quite possible in the present combination of a metallic FSP and a brittle target, specially, if striking velocity exceeds the ballistic limit by more than 5 – 10% [27]. But in nanophased core, another failure mode, that is, radial fracture, is also dominant. In nanophased core, there are several cracks running radially from the periphery of the crater, whereas there is only one



TABLE 2: Experimental data for sandwiches under high-velocity impact.

Material	Striking velocity (m/s)	Residual velocity (m/s)	Mass of projectile (gm)	Energy absorbed per areal density (N-m <sup>3</sup> /Kg)	Ballistic limit per areal density (m <sup>3</sup> /kg-s)
Neat Sandwich	783.95	732.69	13.23	42.94	23.29
	803.80	755.95	13.22	38.38	21.25
	819.35	769.70	12.83	40.74	22.62
Average				40.69	22.39
Nanophased Sandwich	793.75	738.37	13.23	47.06	24.42
	803.80	744.14	13.08	50.36	25.34
	821.15	763.12	12.93	49.56	25.28
Average				48.99	25.02
Gain				20%	12%

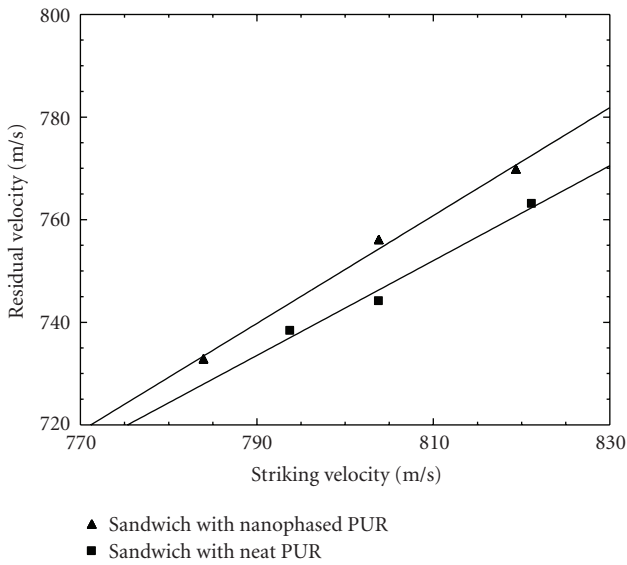


FIGURE 5: Striking velocity versus Residual Velocity Curves for Neat and Nanophased Sandwiches.

crack running radially in case of neat core. Moreover, crack in nanophased foam changes its path as indicated in Figure 6(b) by an elliptical marker. There was also evidence of several cracks changing fracture plane and propagating through thickness in nanophased core. These numerous cracks give nanophased core a progressive failure which left the larger crater at the back side of the nanophased core. It is believed that the stiffer nanoparticle may force the propagating cracks to bow or to branch, to change their direction, and even to change the fracture plane (Figure 6(b), side views). The numerous cracks in nanophased core created a number of new surfaces. This initiates new energy dissipation mechanism in case of nanophased sandwich which explains the overall enhancement in energy absorption.

3.4. High-Speed Photographic Analysis. In order to characterize the ballistic resistance of the neat and nanophased

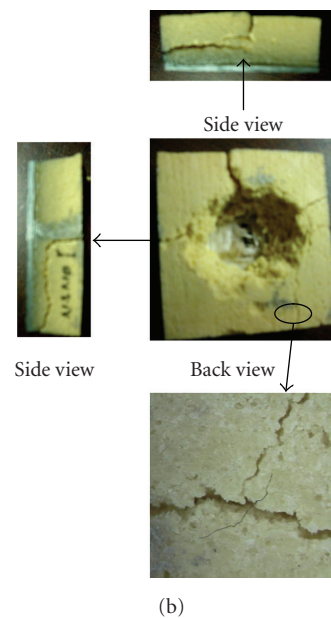
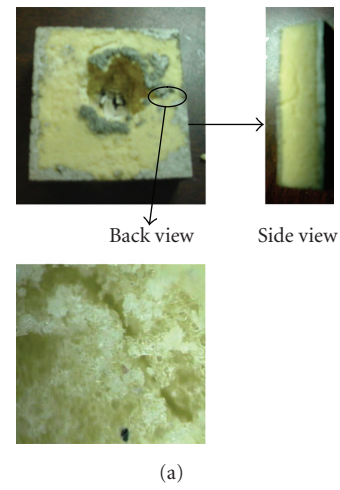


FIGURE 6: Failure modes in (a) neat and (b) nanophased polyurethane cores.

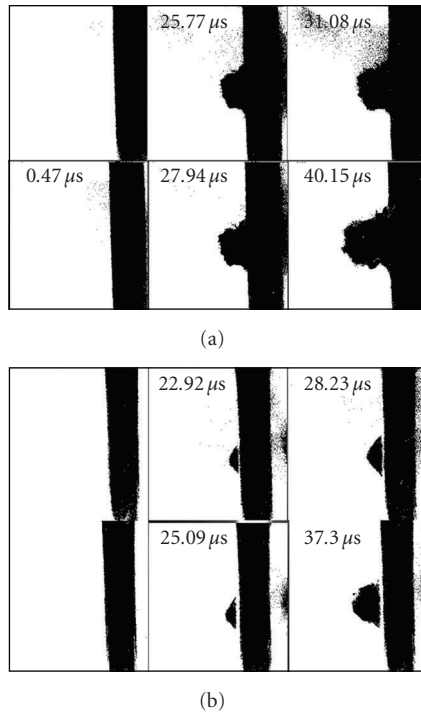


FIGURE 7: High speed photograph (a) neat sandwich (b) nanophased sandwich.

sandwich constructions, it is important to visualize their behavior during the actual impact as the projectile plows through the target. A time-resolved observation of the penetration process can provide a better understanding of the performance. A high-speed Imacon camera (IMACON 468) was used to investigate the deformation process. Figure 7 shows the typical high-speed photograph for neat and nanophased sandwiches. The time in each frame indicates the time after the tip of the projectile touched the front face of the target. As it can be seen from Figure 7(a), for neat sandwich, there is no trace of bulge at the back face in first two frames. The reason is that, in first frame, the projectile did not impact the target yet, and in the second frame, the projectile passed only 0.47 microsecond after the impact. From 3rd frame and onward, the gradual growth of the bulge can be observed. Similar trend can be observed for nanophased sandwich if one looks at Figure 7(b). The projectile needs to be captured just after the penetration in order to determine how long the projectile remained inside the target. But the projectile could not be captured clearly as it was obscured by bulges and debris clouds. However, using Newton's law of motion, an estimated value can be obtained about total time of projectile's residence inside the target from average impact velocity, average residual velocity, and the target's thickness and projectile's length. In the present case, it was approximated as 23.23 microseconds.

Imacon 468 software was also used for quantitative measurement of the bulge height. Figure 8 shows the variation of average bulge height as a function of time for both neat and nanophased sandwich. Figure 8 shows a linear relationship

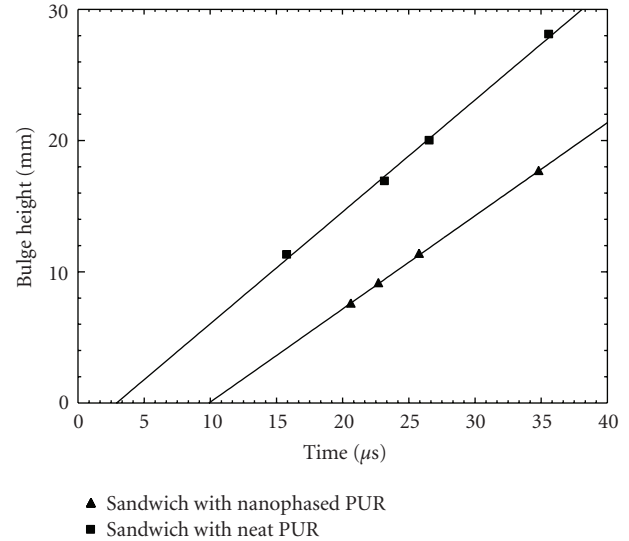


FIGURE 8: Bulge height versus time for sandwiches with both neat and nanophased polyurethane foams.

between the bulge height and the time. This is true for both neat and nanophased sandwich. However, neat sandwich shows larger bulge height than that in nanophased sandwich. The bulging velocity is also slightly higher in neat sandwich as compared to nanophased sandwich. This time-dependent bulge heights data can also be used to predict the critical time for bulge initiation which is one of the important phenomenon to consider during ballistic impact. It was found that the initiation of bulge height had been delayed for nanophased sandwich nearly by 7 microseconds as compared to neat sandwich. This means that the projectile stayed inside the target 7 microseconds longer in nanophased sandwich than the neat one which is about 30% of estimated time of projectile being inside the target.

To further investigate the bulging process of neat and nanophased sandwiches, the bulge contours of both sandwiches are superimposed in Figure 9. The bulge contours were selected from the same time frame ( $\approx 25$  microseconds) for both neat and nanophased sandwiches for better comparison. It is interesting to see that the bulges in neat and nanophased sandwiches exhibited different contours. In neat sandwich, the bulge showed a more or less round contour while it was conical for nanophased sandwich. Though both sandwiches have identical front and back facesheets, they have different core—neat and nanophased. As nanophased core absorbed more energy, the backface of nanophased sandwich was impacted at lower velocity than the neat one. The higher velocity of projectile caused a rigorous failing of the back face of neat sandwich and created comparatively larger and round shape bulge.

#### 4. Summary

In summary, it has been shown that simple dispersion of a small weight percent of  $\text{TiO}_2$  nanoparticles into polyurethane foam can significantly change its cell structures

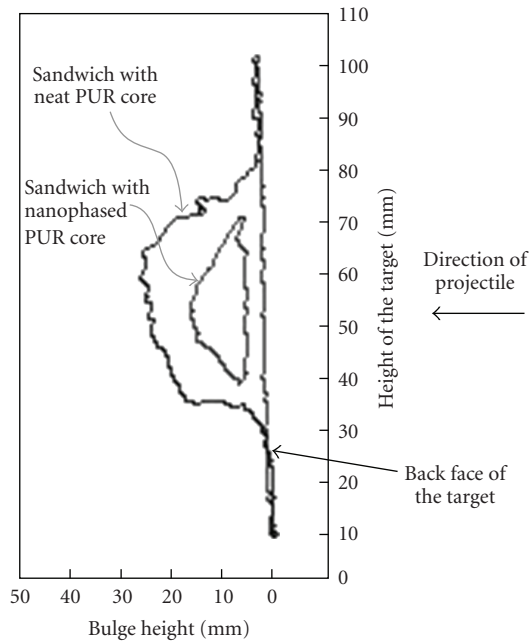


FIGURE 9: Bulge contours of neat and nanophased sandwiches.

and hence affect mechanical properties especially under ballistic loading as investigated here. It is clearly demonstrated that sandwiches with nanophased cores have superior ballistic performance with respect to absorption of kinetic energy as well as in case of ballistic limit. Through digital imaging it is also shown that during its travel through the target the projectile is held longer within the nanophased core due to energy-absorbing failure modes induced by nanoscale inclusions. These failure modes have been identified as fragmentation accompanied with the formation of numerous radial cracks in multiple fracture planes.

## Acknowledgments

The authors would like to acknowledge the Office of Naval Research (Grant no. N00014-90-J-11995) and the National Science Foundation (Grant no. HRD-976871) for supporting this research.

## References

- [1] A. G. Mamalis, D. E. Manolacos, G. A. Demosthenous, and M. B. Ioannidis, *Crashworthiness of Composite Thin-Walled Structural Components*, Technomic Publishing, Lancaster, Pa, USA, 1998.
- [2] A. G. Mamalis, M. Robinson, D. E. Manolacos, G. A. Demosthenous, M. B. Ioannidis, and J. Carruthers, "Crashworthy capability of composite material structures," *Composite Structures*, vol. 37, no. 2, pp. 109–134, 1997.
- [3] M. E. Backman and W. Goldsmith, "The mechanics of penetration of projectiles into targets," *International Journal of Engineering Science*, vol. 16, no. 1, pp. 1–99, 1978.
- [4] S.-W. R. Lee and C. T. Sun, "Dynamic penetration of graphite/epoxy laminates impacted by a blunt-ended projectile," *Composites Science and Technology*, vol. 49, no. 4, pp. 369–380, 1993.
- [5] S. J. Bless and D. R. Hartman, "Ballistic penetration of S-2 glass laminates," in *Proceedings of the 21st International SAMPE Technical Conference*, Atlantic City, NJ, USA, September 1989.
- [6] R. G. Villanueva and W. J. Cantwell, "The high velocity impact response of composite and FML-reinforced sandwich structures," *Composites Science and Technology*, vol. 64, no. 1, pp. 35–54, 2004.
- [7] W. Goldsmith, G.-T. Wang, K. Li, and D. Crane, "Perforation of cellular sandwich plates," *International Journal of Impact Engineering*, vol. 19, no. 5–6, pp. 361–379, 1997.
- [8] W. Goldsmith and J. L. Sackman, "An experimental study of energy absorption in impact on sandwich plates," *International Journal of Impact Engineering*, vol. 12, pp. 241–262, 1992.
- [9] P. H. Bull, S. Hallstrom, and K. A. Olsson, "High velocity impact of large sandwich panels," *Sandwich Construction*, vol. 5, p. 727, 1999.
- [10] M. Uddin, M. Saha, H. Mahfuz, V. Rangari, and S. Jeelani, "Strain rate effects on nanophased polyurethane foams," in *Proceedings of the International SAMPE Technical Conference (SAMPE '04)*, pp. 2309–2322, 2004.
- [11] H. Mahfuz, M. F. Uddin, V. K. Rangari, M. C. Saha, S. Zainuddin, and S. Jeelani, "High strain rate response of sandwich composites with nanophased cores," *Applied Composite Materials*, vol. 12, no. 3–4, pp. 193–211, 2005.
- [12] L. J. Lee, C. Zeng, X. Cao, X. Han, J. Shen, and G. Xu, "Polymer nanocomposite foams," *Composite Science and Technology*, vol. 65, no. 15–16, pp. 2344–2363, 2005.
- [13] X. Cao, L. J. Lee, T. Widya, and C. Macosko, "Polyurethane/clay nanocomposites foams: processing, structure and properties," *Polymer*, vol. 46, no. 3, pp. 775–783, 2005.
- [14] C. Zilg, R. Thomann, R. Mülhaupt, and J. Finter, "Polyurethane nanocomposites containing laminated anisotropic nanoparticles derived from organophilic layered silicates," *Advanced Materials*, vol. 11, no. 1, pp. 49–52, 1999.
- [15] Z. S. Petrović, I. Javni, A. Waddon, and G. Bánhegyi, "Structure and properties of polyurethane-silica nanocomposites," *Journal of Applied Polymer Science*, vol. 76, no. 2, pp. 133–151, 2000.
- [16] I. Javni, W. Zhang, V. Karajkov, and Z. S. Petrovic, "Effect of nano- and micro-silica fillers on polyurethane foam properties," *Journal of Cellular Plastics*, vol. 38, no. 3, pp. 229–239, 2002.
- [17] R. Roy, "Purposive design of nanocomposites: entire class of new materials," *Materials Science Research*, vol. 21, pp. 25–32, 1986.
- [18] Q. Wang, H. Xia, and C. Zhang, "Preparation of polymer/inorganic nanoparticles composites through ultrasonic irradiation," *Journal of Applied Polymer Science*, vol. 80, no. 9, pp. 1478–1488, 2001.
- [19] H. Mahfuz, V. K. Rangari, M. S. Islam, and S. Jeelani, "Fabrication, synthesis and mechanical characterization of nanoparticles infused polyurethane foams," *Composites Part A*, vol. 35, no. 4, pp. 453–460, 2004.
- [20] M. F. Uddin, H. Mahfuz, S. Zainuddin, and S. Jeelani, "Infusion of spherical and acicular nanoparticles into polyurethane foam and their influences on dynamic performances," in *Proceedings of the 6th International Symposium on MEMS and Nanotechnology*, pp. 147–153, SEM, Portland, Ore, USA, June 2005.

- [21] G. J. Price, "Recent developments in sonochemical polymerisation," *Ultrasonics Sonochemistry*, vol. 10, no. 4-5, pp. 277–283, 2003.
- [22] Owens Corning, Toledo, Ohio, USA, 43613.
- [23] "Material Data Sheet: SC-15," Applied Poleramic, Benicia, Calif, USA.
- [24] Utah Foam Product, Nephi, Utah, USA.
- [25] Nanophase Technologies Corporation, Burr Ridge, Ill, USA.
- [26] K. H. Choe, D. S. Lee, W. J. Seo, and W. N. Kim, "Properties of rigid polyurethane foams with blowing agents and catalysts," *Polymer Journal*, vol. 36, no. 5, pp. 368–373, 2004.
- [27] K. Ray, *High Velocity Impact Phenomenon*, Academic Press, New York, NY, USA, 1970.





**Hindawi**

Submit your manuscripts at  
<http://www.hindawi.com>

